SAND2011-5664C

HELIOSTAT FOCAL LENGTH IMPACTS ON SOFAST SENSITIVITY

Julius Yellowhair[1], Charles E. Andraka[2], and Nolan Finch[2]

[1] Sandia National Laboratories, National Solar Thermal Test Facility, P.O. 5800 MS 1127, Albuquerque, NM 87185-1127 USA, 1-505-844-3029, jeyello@sandia.gov

[2] Sandia National Laboratories, National Solar Thermal Test Facility, P.O. 5800 MS 1127, Albuquerque, NM 87185-1127 USA

Abstract

The SOFAST system uses fringe reflection methods to provide a detailed surface normal map of a reflective facet used in concentrating solar power systems. SOFAST was recently extended from short focal length point-focus systems to support heliostat and trough facets. This extension introduced additional variables in the physical set-up of the system. In addition, a large target screen and a short distance between the facet and the screen relative to facet focal length changes the system sensitivities to uncertainties. In characterizing heliostat facets, and in particular when focusing the facets, it is important to understand the uncertainties and sensitivities. In this paper, we explore the sensitivities of the SOFAST system when measuring and focusing heliostat facets of various focal lengths suitable for deployment in our 5 MW_{th} heliostat field at Sandia National Laboratories. We developed test case heliostat facets analytically, with "perfect" surface shapes, and then empirically explore the sensitivities of SOFAST to deviations in the system set-up parameters.

1. Introduction

SOFAST (Sandia Optical Fringe Analysis Slope Tool) uses fringe reflection methods to provide a detailed surface normal map of a reflective facet for CSP systems [1]. It has been used at Sandia National Laboratories (SNL) to measure and align facets in short focal length point-focus systems [2-3]. SOFAST was recently extended from the short focal length point-focus systems to support heliostats facets. The purpose was to set the focus on the facets using the single push/pull screw centered on the backside of the facet; the screw is attached to a circular plate, which is bonded to the backside of the facet [4]. This extension of SOFAST introduced additional variables in the physical set-up of the system. In addition, a large target screen and the short distance between the facet and the screen relative to the facet focal length changes the system sensitivities to uncertainties. In characterizing heliostat facets, and in particular when focusing the facets, it is important to understand the uncertainties and sensitivities. We explore the sensitivities of the SOFAST system when measuring heliostat facets of various focal lengths suitable for deployment in SNL's 5 MW_{th} heliostat field.

The SOFAST version for short focal length point-focus systems uses a flat liquid crystal display (LCD) monitor as a target surface for the display of fringe patterns [1]. The advantage of the LCD monitor is that the pixels are fixed on a regular grid, and the spacing can be inferred from the overall display dimensions. In addition, the camera can be permanently affixed to the monitor, and easily aligned to be perpendicular to the surface of the monitor. These aspects of the set-up remove a number of significant uncertainties from the physical set-up [3]. The nearly-flat heliostat facets require a target screen more than twice the size of the facet to account for the reflected rays from a flat facet plus any surface errors in the facet. We chose to use a LCD projection system and a 3.48 × 2.65 m flat white target screen to measure the 1.22 m square facets. In this paper, we explore the sensitivities of basic set-up parameters on the focal length measurement of two representative analytical sample facets. We developed test case heliostats analytically, with "perfect" surface shapes, and then empirically explore the sensitivities of SOFAST to deviations in the system set-up parameters. For the purposes of measuring and then setting the focal lengths of the facets before deployment, it is important to understand the sensitivities to various set-up parameters of our measurement system.

2. Approach

2.1. SOFAST set-up

Our baseline SOFAST system set-up for measuring heliostat facets is shown in Figure 1. A LCD projector mounted above the set-up projects the fringe pattern onto the screen, and a digital camera mounted by the screen views the fringe pattern in reflection through the heliostat facet being measured. Figure 1a shows a solid model of the set-up, and Figure 1b shows a Matlab [5] model used to generate synthetic data. The target size at the screen is nominally 3.481 (horizontal) × 2.654 (vertical) m; the target size is the display area for the projector. The camera is located -187.7, 35.6, and 4.5 cm from the target center horizontally (x), vertically (y), and in z, respectively. The facet is located 11.2 m from the target and nominally centered on the camera field-of-view (FOV). A 35 mm focal length lens is used with the camera. The camera-lens combination is calibrated using the Cal Tech camera calibration Matlab toolbox [6], which then provides a pinhole model of the camera. The distance parameters are measured with a tape measure, a hand-held laser range finder, and camera extrinsic characterization, instead of expensive survey equipment such as a theodolite or a laser tracker. These measured set-up parameters were imported into our software to generate the synthetic data.

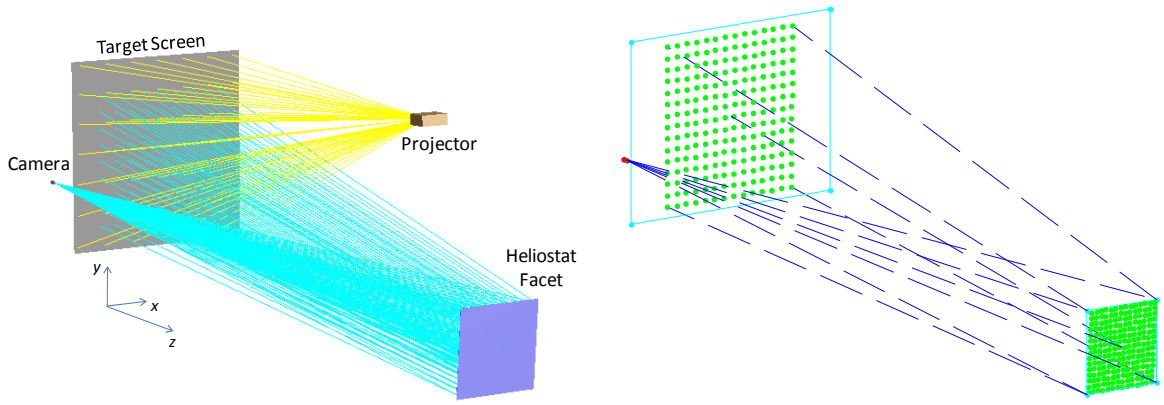

(a) (b)

Fig. 1. Baseline SOFAST set-up to measure heliostat facets. (a) A solid model of the set-up, and (b) a Matlab model used to generate the synthetic data.

2.2. Analytical facet

The SNL heliostat facets are 1.22 m (48 in) square, as are the generated analytical facets used in this study. The analytical facet surfaces were shaped to a sphere with radius of curvature equal to twice the facet focal length. The focal lengths were set to 100 and 250 m, which correspond to the mid and maximum slant ranges of SNL's heliostat field to the receiver tower. Using the measured physical set-up parameters, the modeled components (camera, facet, and screen) were placed in the analytical model. Rays were then generated from pixels on the camera focal plane array, through the camera pinhole, reflected off the analytical facet surface and intersected with the target screen. The coordinates of the intersection points (from the reflected rays) at the target screen along with the physical set-up parameters were input into SOFAST for analysis of the facet. The analytical model of the camera used an ideal 35 mm lens (i.e. with no distortions).

2.3. Key variables

A large number of physical set-up parameters must be determined in the SOFAST system. We identified some physical set-up parameters that appear to have a profound effect on the facet focal length measurement. To determine the focal length on a measured facet, we start with a parabolic model of the facet shape,

$$z = Ax^2 + By^2 + Cx + Dy + Exy + F\,. \tag{1}$$

Points on the facets are converted to surface normals and are then expressed as surface slopes in the x and y directions in the facet coordinate frame,

$$s_x = \frac{\partial z}{\partial x} = 2Ax + C + Ey$$
$$s_y = \frac{\partial z}{\partial y} = 2By + D + Ex \quad . \tag{2}$$

The facet surface normals are determined from first knowing the location of the camera entrance pupil, **C**(*x*,*y*,*z*), relative to the facet location. The focal plane of the camera (projected through the camera pinhole) is then mapped onto the facet surface, so the points **C**(*x*,*y*,*z*) and **F**(*x*,*y*,*z*) are known (i.e. 'rays' generated from pixels on the camera focal plane go through the center of the camera entrance pupil and intersected with the facet surface). The 'rays' that connect these points reflect off the facet and intersect the screen surface or the target. In a real SOFAST measurement, the screen intersection points, **S**(*x*,*y*,*z*), are accurately determined from the fringe reflection techniques. With our synthetic data, **S**(*x*,*y*,*z*) are determined analytically using the law of reflection at the facet surface and by intersecting the reflected 'rays' with a flat plane representing the target screen. From the law of reflection, the incident ($\overline{\mathbf{FC}_i}$) and reflected ($\overline{\mathbf{SF}_i}$) 'rays' form angles at the facet as shown in Figure 2. The bisectors of the angles are the facet surface normals, which are converted to surface slopes.

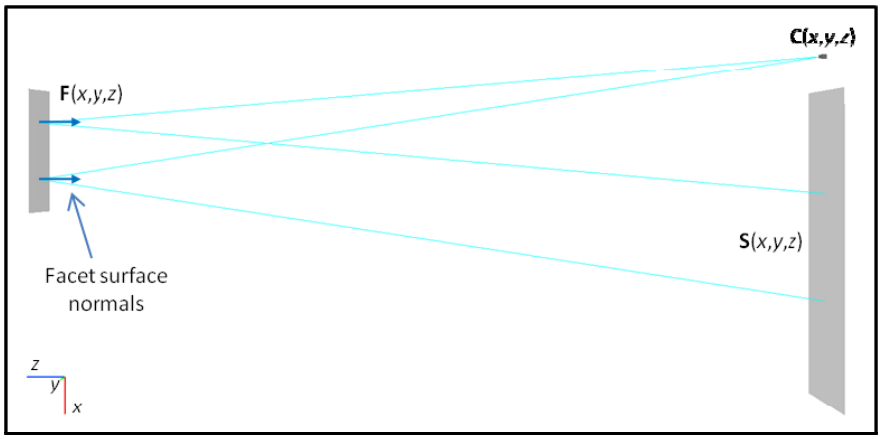

Fig. 2. Determination of the facet surface slopes. A top view of the set-up is shown.

The first partial derivatives (Eqn. 2) of our parabolic model (Eqn. 1), or slope functions, are then fit to the facet slope data in a least-squares sense. The fit coefficients of the linear terms (*A*, *B*) of the slope functions are related to the focal length in the *x* and *y* directions by

$$f_x = \frac{1}{4A}$$
$$f_y = \frac{1}{4B} \quad . \tag{3}$$

Uncertainties in the physical set-up parameters affect the focal length calculation. These uncertainties and their impacts must be understood when measuring and setting the focus of heliostat facets. We selected to vary the camera position, facet location in *z*, and target dimensions in this sensitivity study. We looked at the effects of these key parameters on the measured focal length for facets with 100 and 250 m nominal focal lengths. We recognized that the influence of uncertainty in these areas may have a varying influence on the measurement as the focal length becomes very long relative to the measurement system.

2.4. Effect of measurement errors on key variables

Figure 3 depicts the SOFAST set-up to measure heliostat facets with the distances between the components shown. Note that in this study, SOFAST was not used to collect data on real facets; instead synthetically generated data are used, and the analysis package of SOFAST is used to analyze the synthetic data. The key studied variables in the set-up are the camera relative position from the target center, the target dimensions,

and the facet center to target center distance.

2.4.1. Measurement error on camera position

The location of the camera entrance pupil (EP) relative to the target center is measured with a standard tape measure. Standard tape measures are inherently limited in accuracy. The separation distance between the target center and the camera is relatively large, so slack in the tape measure can affect the distance measurement. In addition, the location of the camera entrance pupil is located somewhere within the lens barrel of the camera. Its location is estimated from the lens and mechanical design layout acquired from the manufacturer. These sources of error contribute to the total measurement error of the distance between the camera EP position and the target center.

Figure 4 schematically shows the error in measuring the camera EP position as a shift of the point **C**. The dashed lines are deviations from the nominal camera EP location (solid lines). The distances between the point **C** and all the points on the facet, **F**, are not constant. Therefore, a shift in the point **C** (due an error in measurement) will not shift the calculated facet surface normals uniformly across the facet. The result is an error in the calculated facet focal length.

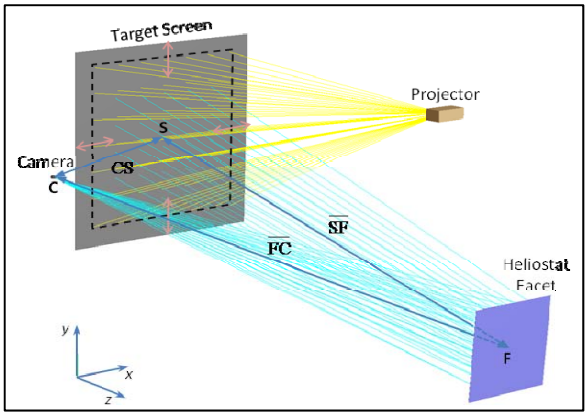

Fig. 3. SOFAST set-up for measuring heliostat facets with the distances between components shown.

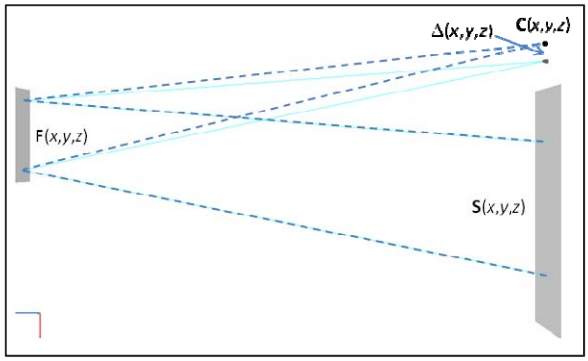

Fig. 4. Schematic showing the effect of an error in measuring the camera position in *x*, *y*, and *z* on the facet surface normal calculation (top view of the set-up).

2.4.2. Measurement error on facet position

The location and orientation of the facet relative to the camera is initially estimated through an extrinsic characterization, which uses a homography process, where the camera captures an image of the facet and the software performs an analysis of the facet image. The lens model from the camera-lens calibration is used to make the real camera act like a pinhole. The extrinsic calibration software returns a reversible six element position/orientation vector. The distance from the facet center to the target center is then measured with a hand-held laser range finder (LRF) as shown in Figure 5.

The extrinsic characterization can be limited in accuracy due to various error sources (e.g. facet corner detection accuracy, lens calibration accuracy, *etc*.). Since the separation between the camera EP and target center is measured directly, the distance between the camera and the facet center estimated from the extrinsic characterization can be verified with a measurement from the facet center to the target center. Additional measurements from the facet center to known points on the target provide additional constraints to the facet location. The points **C**, $\mathbf{F_0}$, and $\mathbf{S_0}$ form a triangle, where $\mathbf{F_0}$ and $\mathbf{S_0}$ are points on the facet center and target center, respectively. The sides of the triangle are measured with different tools. To form the proper triangle, the measured sides must agree reasonably well. If the distances measured do not provide a reasonable solution on the triangle, then the distance measured by the extrinsic characterization is updated. The distances $\mathbf{S_0F_0}$ and $\mathbf{CS_0}$ are kept constant, while the distance $\mathbf{F_0C}$ (from homography) is re-adjusted to get a reasonable solution. If there is an error in measuring the facet center to target center distance, this error causes all the points **F** to shift towards or away from the camera along the camera optical axis, due to the re-adjustment of the distance $\mathbf{F_0C}$ initially calculated using homography. Figure 6 shows an example of an

under-estimation of the facet to target distance. The dashed lines represent rays deviated from the nominal rays (solid lines).

2.4.3. Measurement error on target dimensions

The dimensions of the target (screen display area) are also measured with a tape measure. As mentioned previously, the standard tape measures are inherently limited in accuracy, and the target dimensions are large enough that the slack in the tape measure can affect the measurements. Error in the target dimension measurements artificially shrinks or stretches the target size. This effect linearly scales the target intersection points in *x* and *y* (i.e. the target distortion is linear). Figure 6 shows an example of an over-estimation of the target dimension in the horizontal direction (note that the figure shows a top view of the set-up). The intersection points at the target are shifted out accordingly (dashed lines). Consequently, the surface normals will be gradually shifted outward, resulting in an over-estimation of the facet focal length (i.e. the calculated focal length will be longer) since the target screen is located inside the focus of the facets being measured. Similarly, an under-estimation of the target dimension will result in shorter calculated facet focal lengths, if the target screen is located inside the facet focus.

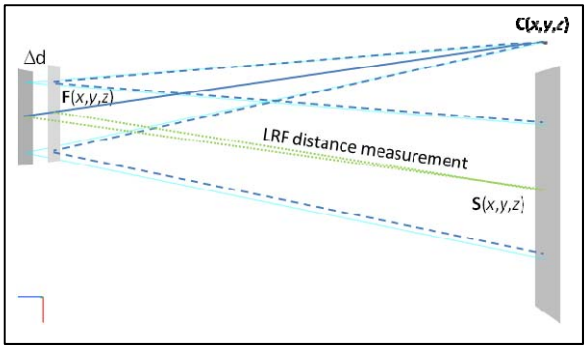

Fig. 5. Schematic showing an example of a facet shift due an error in the distance measurement between the facet center and the target center (top view).

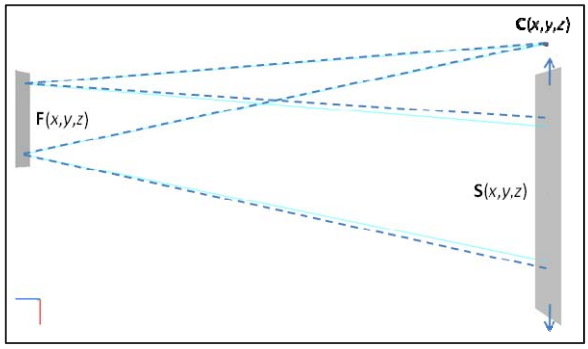

Fig. 6. Schematic showing an example of an over-estimation of the target dimensions in the horizontal direction (top view).

2.5. Sensitivity analysis method

Different methods are available (e.g. Monte Carlo, finite difference *etc*.) for performing sensitivity analyses of systems [7]. In a Monte Carlo approach, probability distributions of the variables over a defined domain are first determined. Then multiple runs, or simulations, are performed while randomly sampling the distributed variables with each run. We chose, instead, to use the finite difference approach. In the finite difference approach, the variables are individually varied over the defined domains (e.g. ±1 mm) and the behavior of the system (e.g. facet focal length calculation sensitivity) is observed for each parameter. This method then predicts performance sensitivity for each parameter, which helps to identify individual parameters that have high sensitivities on system performance. Steps can then be taken to better control the tolerances on the highly sensitive parameters. To predict the total system performance, the individual sensitivity results can be combined.

To follow the finite difference process, we first ran the analysis package of SOFAST on the synthetic data with the nominal values of the physical set-up parameters. The result of the first run showed that SOFAST correctly estimated the focal lengths of the analytical facets. After this validation, we changed the value of one parameter to ±1 mm from the nominal value, and then re-ran the SOFAST analysis and observed the changes in the calculated facet focal length. We repeated the steps for the rest of the variables. For small changes in the variables, except for the target dimensions, the sensitivities appeared to be linear.

3. Results

3.1. Focal length sensitivity analysis

The plot in Figure 7 shows the results of the sensitivity analysis. The focal length sensitivities to variations in the physical set-up parameters are shown. From this plot we can see two things: first, the parameters provide different sensitivity magnitudes, and second, the sensitivities increase dramatically for longer facet focal lengths.

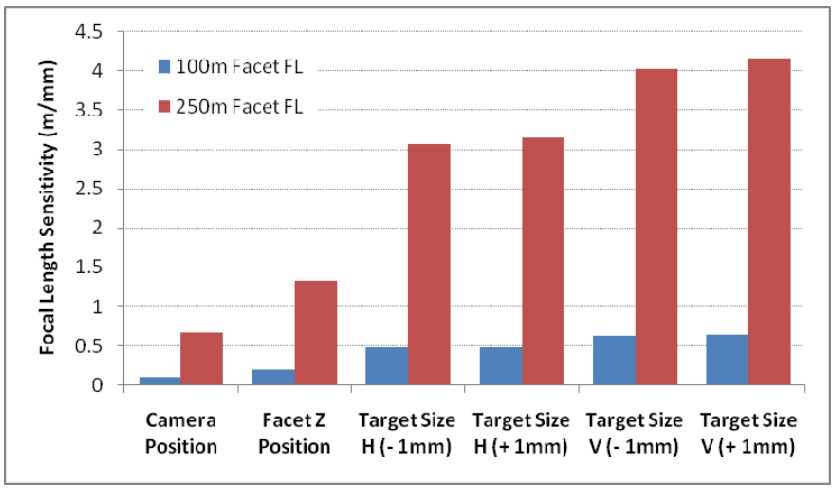

Fig. 7. Measured facet focal length sensitivity to various measurement (SOFAST) set-up parameters.

The first observation is that the errors in the camera position are the least sensitive. For example, a measurement error in the camera position by 1 mm in any direction will cause an error in the focal length calculation by < 1 m for both the 100 and 250 m focal length facets. Variations in the facet *z* position provide moderate sensitivities. A 1 mm error in the facet *z* position results in a focal length error of < 0.5 m for the 100 m facet, but results in a focal length error of about 1.4 m for the 250 m facet. Of the variables studied, measurement errors on the target dimensions are the most sensitive. Here we show the sensitivities for both the ±1 mm variations of the target dimensions, because we determined that over that domain the sensitivities were not linear. For this specific set-up geometry, the -1 mm error appeared to be slightly less sensitive than the + 1mm error. Although ±1 mm errors results in focal length errors of < 1 m for 100 m facets, the focal length errors increase greatly to > 3 m for 250 m facets. With this information, we can place appropriate tolerance bands on each parameter.

The second observation of Figure 7 is that the sensitivity increases greatly for longer focal length facets, especially for variations in the target size. Setting tolerances on the parameters then becomes dependent also on the target focal length of the facets (i.e. tighter tolerances are needed for longer focal length facets). In Section 4, we discuss why the facets with less curvature (i.e. long focal lengths) are more sensitive to changes in slopes across the facet.

3.2. Focal length error impacts on spot size

While the focal length changes were more for longer focal length facets, we wanted to see the net impact on the spot size at the receiver tower. For changes in the facet focal lengths, we looked at the corresponding changes in spot sizes. In particular, we provide the results here for the case of a ±1 mm measurement error in the vertical target dimension. In Figure 8, we plot the focal length against the changes in the focal lengths for this measurement error. A -1 mm measurement error on the target dimension shortens calculated the focal length (i.e. the change is negative), but note that the absolute changes in the focal lengths are plotted in Figure 8a in meters. Also plotted are the corresponding spot size changes (in cm) due to the focal length shifts. Figure 8b is the same plot as 8a but reported in percent changes to better visualize the impacts of the focal lengths errors on the spot sizes. From this analysis, we found that the effect on the focal length is

somewhat mitigated by the reduction of the sensitivity of the spot size on the focal length with increasing focal length. That is, the focal length changes are higher at long focal lengths, but the changes in spots do not increase much with focal length.

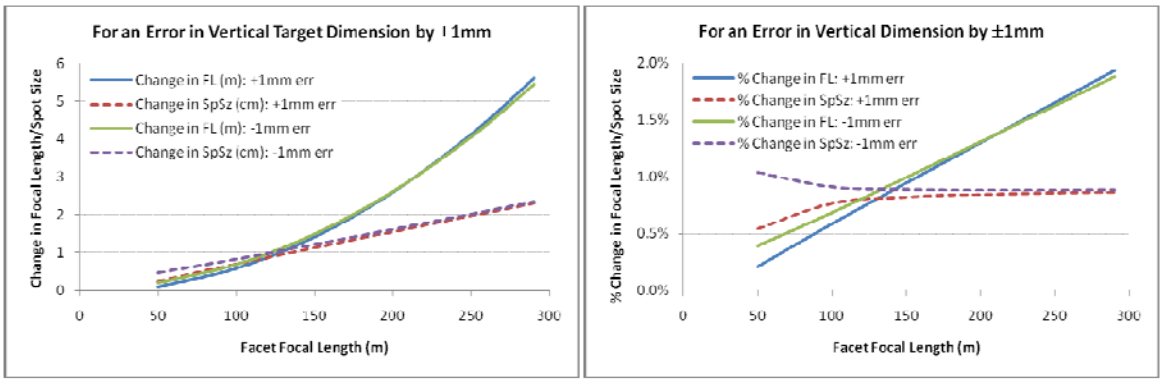

(a) (b)

Fig. 8. Shifts in focal lengths and corresponding spot size variations for a measurement error in the vertical target dimension by ±1 mm, shown as (a) physical changes and (b) percentage changes.

4. Discussion

Given a facet with a smaller curvature (i.e. longer focal length), specified changes in curvature impact the facet focal length to a greater extent. Figure 9 shows, for a 1.22 diameter facet, the difference in sensitivities to curvature changes (plotted in terms of slope changes) at the facet edge for the 100 m (short) and 250 m (long) focal length facets. For the same amount of slope changes at the edge, the longer focal length facets experience much larger focal length changes. This leads to higher uncertainties when measuring the longer focal length facets, but in the field this effect seems to be mitigated by the reduction in sensitivity to spot size.

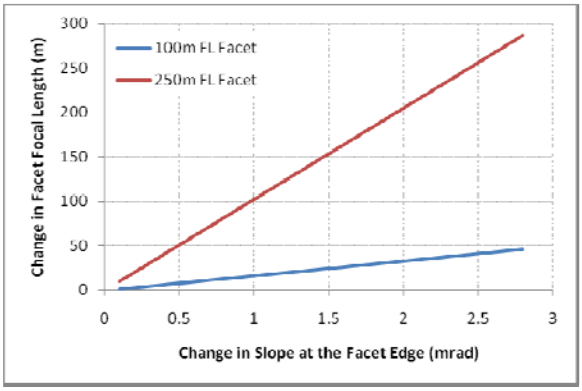

Fig. 9. Facet focal length sensitivity to slope changes at the edge of the facet for a 1.22 m diameter facet.

We must caution that the sensitivity analysis provided here is specific to the set-up geometry used to measure and for the purpose of focusing the SNL heliostat facets. In Section 2.1, we discussed the set-up geometry and provided some specific dimensions and locations of components. The sensitivities may be different for other baseline measurement set-ups, but the trend in the sensitivities should be the same regardless of the set-up geometry (i.e. errors in measuring the target dimensions will be more sensitive than errors in measuring the camera position, for example) [3].

5. Conclusion

SOFAST was initially designed to measure facets of short focal length point-focus concentrators, where it is practical to measure at the '2f' location. We adapted it to measure long focal length heliostat facets with

some changes to the physical set-up parameters and the target screen size. The purpose of this effort was to focus the SNL heliostat facets to the correct slant range using the single push-pull screw adjustment on the backside of the facets. This extension introduced additional variables in the physical set-up of the system. In addition, a large target screen and a short distance between the facet and the screen relative to facet focal length changed the system sensitivities to uncertainties. Lastly, to keep SOFAST simple, we used simple measurement tools to measure the physical set-up parameters, which introduced measurement errors. We studied the focal length impacts on the SOFAST sensitivity on a few key input parameters: camera position, facet *z* position, and target dimensions.

The results of the sensitivity analysis showed that, of all the parameters considered, errors in measuring the target dimensions dominated. This effect linearly scales the points on the target causing an error in the focal length calculation. A similar effect, not discussed in this paper, is distortion of the projected images on the target screen caused by the distortions in the projector lens and positioning of the projector relative to the screen. In this case, the spatial scaling of the points may not be linear. Discussions on the screen distortion errors in the SOFAST set-up can be found elsewhere [7].

The analysis also showed that focal length uncertainty increases dramatically with focal length. For the same amount of slope changes at the edge of the facet, the longer focal length facets experience bigger changes in focal length. However, we found that this effect is somewhat mitigated by the reduction of the sensitivity of the spot size on the focal length with increasing focal length.

Acknowledgements

Sandia National Laboratories is a multi-program laboratory managed and operated by Sandia Corporation, a wholly owned subsidiary of Lockheed Martin Corporation, for the U.S. Department of Energy's National Nuclear Security Administration under contract DE-AC04-94AL85000. The United States Government retains and the publisher, by accepting the article for publication, acknowledges that the United States Government retains a non-exclusive, paid-up, irrevocable, world-wide license to publish or reproduce the published form of this manuscript, or allow others to do so, for United States Government purposes.

References

[1] Andraka, C. E., Sadlon, S., Myer, B., Trapeznikov, K., Liebner, C. (2009). Rapid Reflective Facet Characterization using Fringe Reflection Techniques, *Proceedings of AMSE ES2009*, San Francisco, CA USA, July 19-23.

[2] Andraka, C. E., Yellowhair, J., Trapeznikov, K., Carlson, J., Myer, B., Stone, B., Hunt, K. (2011). AIMFAST: An Alignment Tool Based on Fringe Reflection Methods Applied to Dish Concentrators, Solar Energy 133, 031018.

[3] Finch, N., Andraka, C. E. (2011). Uncertainty Analysis and Characterization of the SOFAST Mirror Facet Characterization System, *Proceedings of ASME ES2011*, Washington, DC, August 07-10.

[4] Andraka, C. E., Yellowhair, J., Finch, N., Ghanbari, C., Chavez, K., Sproul, E. (2011). SOFAST Facet Characterization for Heliostats: Extensions and Difficulties, *Proceedings of SolarPACES*, Granada, Spain, September 20-23.

[5] *MATLAB and Simulink for Technical Computing* (2011). Retrieved from http://www.mathworks.com

[6] Bouguet, J-Y (2010). *Camera Calibration Toolbox for MATLAB.* Retrieved from http://www.vision.caltech.edu/bouguetj/calib_doc/

[7] Frieden, B. R. (2001). *Probability, Statistical Optics, and Data Testing – A Problem Solving Approach* (3rd ed.). New York: Springer-Verlag.